

Topological phase transition driven by magnetic field and topological Hall effect in an antiferromagnetic skyrmion lattice

M. Tomé^{1,2} and H.D. Rosales^{1,2,3}

¹*Instituto de Física de Líquidos y Sistemas Biológicos (IFLYSIB), UNLP-CONICET, Facultad de Ciencias Exactas, La Plata, Argentina*

²*Departamento de Física, Facultad de Ciencias Exactas, Universidad Nacional de La Plata, La Plata, Argentina*

³*Departamento de Cs. Básicas, Facultad de Ingeniería, Universidad Nacional de La Plata, C.C. 67, 1900 La Plata, Argentina*

(Dated: February 2, 2021)

The topological Hall effect (THE), given by a composite of electric and topologically non-trivial spin texture is commonly observed in magnetic skyrmion crystals. Here we present a study of the THE of electrons coupled to antiferromagnetic Skyrmion lattices (AF-SkX). We show that, in the strong Hund coupling limit, topologically non-trivial phases emerge at specific fillings. Interestingly, at low filling an external field controlling the magnetic texture, drives the system from a conventional insulator phase to a phase exhibiting THE. Such behavior suggests the occurrence of a topological transition which is confirmed by a closing of the bulk-gap that is followed by its reopening, appearing simultaneously with a single pair of helical edge states. This transition is further verified by the calculation of the Chern numbers and Berry curvature. We also compute a variety of observables in order to quantify the THE, namely: Hall conductivity and the orbital magnetization of electrons moving in the AF-SkX texture.

PACS numbers:

Introduction.— Magnetic skyrmions, a kind of topologically protected solitons, are nanometer size spin textures that have shown to be of great practical interest due both to the fundamental properties and its promising potential in spintronics based applications[1, 2]. They have been evidenced experimentally in a wide variety of materials including chiral magnets such as MnSi [3, 4], FeGe [5], Fe_xCo_{1-x}Si [6] and β -Mn-type Co-Zn-Mn [7]; and insulator materials as Cu₂OSeO₃[8, 9]. In most cases, periodic arrays of skyrmions are stabilized by the competition of strong ferromagnetic exchange interactions, external magnetic field and the antisymmetric Dzyaloshinskii-Moriya (DM) interaction [10–13]. However, in recent years, theoretical studies have suggested that skyrmions might be also stabilized in antiferromagnets where frustration helps to stabilize antiferromagnetic skyrmions crystals (AF-SkX) consisting of multiple interpenetrated ferromagnetic Skyrmion lattices [14–22]. Recently, in the spinel MnSc₂S₄ the first realization of an AF-SkX (fractional) like-structure has been discovered, where the planes (triangular lattices) perpendicular to the field direction host interpenetrated fractional ferromagnetic Skyrmion lattices [23].

When conduction electrons are coupled to the local magnetic background, they accumulate a Berry phase as they travel through skyrmions spin configuration which acts as a local effective magnetic field leading to topological Hall effect (THE) [24–31]. Most of the previous studies on THE have focused on systems consisting of ferromagnetic SkX showing unconventional behaviour that emerges as a consequence of the non-trivial smooth magnetic texture [32–34]. However, a not so desired feature

of skyrmions hosted in ferromagnets is that they exhibit an inevitable topology effect, namely, the skyrmion Hall effect [35]. In this phenomena, the magnetic skyrmions do not move collinear to the current flow direction, but acquire a transverse motion due to the appearance of a topological Magnus force acting upon the non-zero topological charge. To avoid this disadvantage, theoretical studies have suggested that the skyrmion Hall effect can be suppressed by utilizing the counterpart of the ferromagnetic skyrmions: the antiferromagnetic skyrmions, which are also topologically protected but without showing the skyrmion Hall effect [36]. In this context, electrons coupled to antiferromagnetic skyrmion lattices AF-SkX have been less explored, even knowing that the multiple sublattice structure can induce interesting magnetic phenomena [37]. Therefore a question that arises naturally is whether conduction electrons coupled to this kind of skyrmion lattices could present exotic new physics.

This letter address this relevant question on the THE of electrons in topologically non-trivial AF-SkX textures on the triangular lattice. By means of extensive Monte-Carlo simulations and exact diagonalization for the magnetic and fermionic sector respectively, we find that in the strong Hund coupling limit, at low filling it is possible to control the THE and its protected edge states by tuning the external magnetic field. This phenomena is confirmed by a closing and further reopening of the bulk-gap and the transition from trivial to non-trivial Chern number. As a complement, we have computed the orbital magnetization, which is directly related to Berry-phase effect, showing surprisingly opposite signs at both sides of the topological transition. This property enables

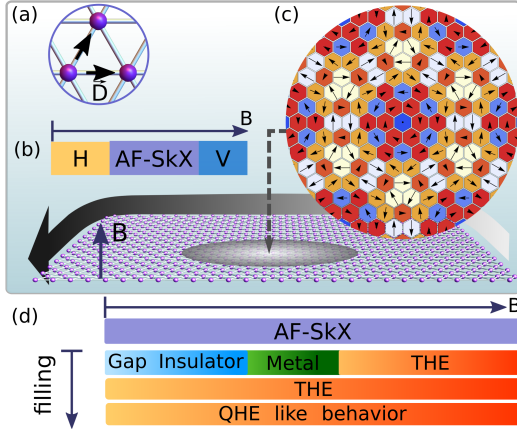


FIG. 1: (Color online) (a) DM interactions \mathbf{D} (black arrows). (b) Low temperature phase diagram of the magnetic Hamiltonian in Eq. (2) including Helical (H), AF-SkX and vortex like (V) phases. (c) Portion of an AF-SkX magnetic background considered in this paper for $D/J = 0.5$ and $B/J = 4.6$. (d) Schematic phase diagram of the electronic Hamiltonian in Eq. (3). At low filling, the magnetic field induces a sequence of topological transitions: band insulator \rightarrow metal \rightarrow THE; at high filling the system's behaviour can be connected with Integer Quantum Hall Effect.

a “switch” on/off of the THE and orbital magnetization by an external magnetic field.

Model and Methods.— In this work we consider a tight-binding model on a triangular lattice where the interaction of electrons with an AF-SkX texture is described by the Hamiltonian,

$$H = - \sum_{\langle \mathbf{r}, \mathbf{r}' \rangle, \sigma} t_{\mathbf{r}\mathbf{r}'} (\hat{c}_{\mathbf{r}\sigma}^\dagger \hat{c}_{\mathbf{r}'\sigma} + \text{h.c.}) - J_h \sum_{\mathbf{r}, \mu\nu} \mathbf{S}_{\mathbf{r}} \cdot \mathbf{s}_{\mathbf{r}} \quad (1)$$

where $\hat{c}_{\mathbf{r}\sigma}$ ($\hat{c}_{\mathbf{r}\sigma}^\dagger$) is the creation (annihilation) operator at the site \mathbf{r} with spin ($\sigma = \uparrow, \downarrow$), $t_{\mathbf{r}\mathbf{r}'}$ is the hopping between nearest-neighbor sites, J_h is the Hund's coupling strength between the electron spin $\mathbf{s}_{\mathbf{r}} = \frac{1}{2} \hat{c}_{\mathbf{r},\mu}^\dagger \boldsymbol{\sigma}^{\mu\nu} \hat{c}_{\mathbf{r},\nu}$ and magnetic background $\mathbf{S}_{\mathbf{r}}$. In order to include a spin texture made of an AF-SkX phase we perform Monte Carlo simulations with overrelaxation updates [14, 38] for system sizes of $N = L^2$ sites ($L = 12 - 84$) and periodic boundary conditions on the following pure magnetic Hamiltonian [14, 39] (see Supplemental Material [40], Sec. I, for more details on the simulations).

$$H_S = \sum_{\langle \mathbf{r}, \mathbf{r}' \rangle} J \mathbf{S}_{\mathbf{r}} \cdot \mathbf{S}_{\mathbf{r}'} + \mathbf{D}_{\mathbf{r}\mathbf{r}'} \cdot (\mathbf{S}_{\mathbf{r}} \times \mathbf{S}_{\mathbf{r}'}) - B \sum_{\mathbf{r}} S_{\mathbf{r}}^z \quad (2)$$

where J and $\mathbf{D}_{\mathbf{r}\mathbf{r}'} = D(\mathbf{r}' - \mathbf{r})/\|\mathbf{r}' - \mathbf{r}\|$ are the antiferromagnetic and DM nearest neighbour couplings respectively (see Fig. 1a), and B the strength of the magnetic field along the z axis. We will consider $D/J = 0.5$ for the rest of the paper as a representative value [14, 39] where it is known that from the model in Eq. (2) emerges

a AF-SkX consisting of the superposition of three interpenetrated ferromagnetic skyrmion lattices [14, 39] (Fig. 1c) correspond to a portion of the lattice for $B/J = 4.6$. See Supplemental Material [40], Sec. I.

In a recent work it was shown that the mixed dynamics of both electrons and spins tend to stabilize the AF-SkX phase in the adiabatic regime $J_H/t \gg 1$ [41] allowing us to fix the magnetic texture in Eq. (1) throughout our calculations. With this in mind, let's focus in this regime $J_H/t \gg 1$ where the spin of the electrons are aligned parallel to the local moment and the low-energy physics can be described by an effective Hamiltonian of spinless fermions as [42] (see Supplemental Material [40], Sec. II for details).

$$H_{eff} = \sum_{\mathbf{r}, \mathbf{r}'} t_{\mathbf{r}\mathbf{r}'}^{eff} \hat{d}_{\mathbf{r}}^\dagger \hat{d}_{\mathbf{r}'}, \quad (3)$$

where $\hat{d}_{\mathbf{r}}^\dagger$ ($\hat{d}_{\mathbf{r}}$) is the creation (annihilation) operator, $\cos \theta_{\mathbf{r}\mathbf{r}'} = \mathbf{S}_{\mathbf{r}} \cdot \mathbf{S}_{\mathbf{r}'}$, $t_{\mathbf{r}\mathbf{r}'}^{eff} = t_{\mathbf{r}\mathbf{r}'} \cos(\theta_{\mathbf{r}\mathbf{r}'}/2) e^{i a_{\mathbf{r}\mathbf{r}'}}$ is the effective hopping amplitude and the phase $\tan(a_{\mathbf{r}\mathbf{r}'}) = -\sin(\phi_{\mathbf{r}} - \phi_{\mathbf{r}'})/(\cos(\phi_{\mathbf{r}} - \phi_{\mathbf{r}'}) + \cot(\theta_{\mathbf{r}}/2) \cot(\theta_{\mathbf{r}'}/2))$.

The electronic band structure and other quantities of interest are obtained through numerical diagonalization of the resulting Hamiltonian matrix in the reciprocal space. Therefore, once the eigenvector $|u_n(\mathbf{k})\rangle$ and eigenenergies $\epsilon_n(\mathbf{k})$ are determined, we calculate the Hall conductivity σ_{xy} by means of the standard Kubo formula, which at $T = 0$, reduces to

$$\sigma_{xy} = \frac{e^2}{2\pi\hbar} \sum_n \int \Theta(\epsilon_n - \epsilon_F) \Omega_{xy}^{(n)} d^2k \quad (4)$$

where the Berry curvature for the band n is $\Omega_{ab}^{(n)} = 2 \sum_{m \neq n} \text{Im}\{[v_a]^{nm} [v_b]^{mn}\} / (\epsilon_m - \epsilon_n)^2$, ϵ_F is the Fermi energy and $[v_a]^{nm} = \langle u_n | v_a | u_m \rangle$ ($a = x, y$) is the matrix element of the velocity operator $\mathbf{v} = \frac{i}{\hbar} [H_{eff}, \mathbf{R}]$, with the position operator being $\mathbf{R} = \sum_{\mathbf{r}} \mathbf{r} \hat{d}_{\mathbf{r}}^\dagger \hat{d}_{\mathbf{r}}$. When the Fermi energy ϵ_F lies inside a band gap, the Hall conductivity is quantized as $\sigma_{xy} = e^2/h \sum_n C_n$, where the integers C_n are the so-called Chern numbers. Relevant Chern numbers are calculated independently of σ_{xy} through the Fukui-Hatsugai numerical method [43, 44]. Thus, due to the bulk-boundary correspondence principle [45], in an open-boundary system one would expect to find a number $|\nu|$ of topologically protected chiral edge states crossing the n th band gap, where $\nu = \sum_n C_n$. In addition, we also calculate the out-of-plane component of the orbital magnetization [46–48]

$$\begin{aligned} \mathcal{M}^z &= \mathcal{M}_c + \mathcal{M}_t \\ &= \frac{1}{(2\pi)^2} \sum_n \int_{BZ} \Theta_n m_n^z d^2k \end{aligned} \quad (5)$$

$$+ \frac{e}{4\pi\hbar} \sum_n \int_{BZ} \Theta_n(\Omega_{xy}^{(n)} - \Omega_{yx}^{(n)}) (\epsilon_F - \epsilon_n) d^2k$$

where $\Theta_n = \Theta(\epsilon_n - \epsilon_F)$ is the Heaviside step function, $m_n^c = -\frac{e}{2\hbar} \sum_{m \neq n} \epsilon^{abc} \text{Im}\{[v_a]^{nm} [v_b]^{mn}\} / (\epsilon_m - \epsilon_n)$ is the crystal orbital magnetic moment with ϵ^{abc} is the Levi-Civita tensor (summation over a, b is implicit). \mathcal{M}_c correspond to the contribution from the intrinsic orbital moment (conventional part), whereas \mathcal{M}_t corresponds to corrections of topological nature.

Band Structure and Topological Phase Transition.— In Fig. 2a we show a typical band structure obtained in the presence of an AF-SkX background. Here we identify two main distinct energy regions: (i) a low-energy sector consisting of strongly overlapping bands except for a field dependent global bulk gap Δ_1 between the first and second band (red curves), and (ii) a high-energy sector resembling a typical THE spectrum in the presence of a ferromagnetic Skyrmion background [32] (blue curves). Both sectors are separated by a persistent energy gap Δ_2 (see Fig. 1c).

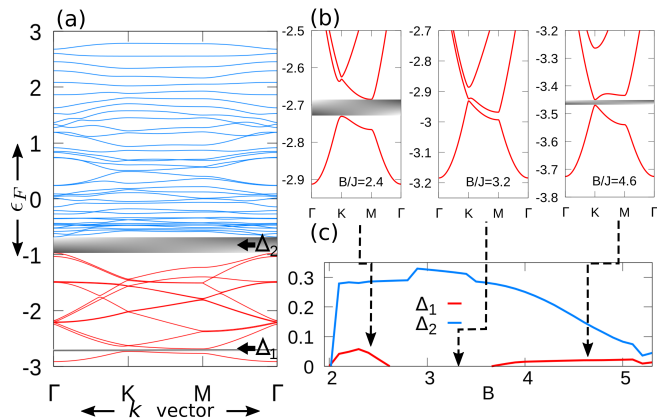


FIG. 2: (Color online) (a) Representative band structure of the model in Eq.(3) for $B/J = 2.4$ (energy in units of t). Red and blue set of curves indicate the two regions with different properties. The gray shaded areas mark the two relevant gaps of the system. (b) Closing and further reopening of the bulk-gap Δ_1 . (c) Evolution of the gaps Δ_1 and Δ_2 vs magnetic field B .

In this section, we focus our attention on the low-energy sector, leaving the discussion for the high energy sector to the next section. For sequentially bigger fields it is found that the overlapping region barely changes. Fig. 2(b) shows a closing and further reopening of the first bulk gap Δ_1 for increasing fields. These two sectors where Δ_1 is non-zero (at low field and a high field) are well separated by a broad gapless region as shown in Fig. 2(c). Upon further inspection we find a noticeable change in both the Hall conductivity and orbital magnetization when the Fermi energy sits inside the band gap. In Fig. 3 we show this quantities for low field (left) and high field (right) displaying a transition from $\sigma_{xy} = 0$ at

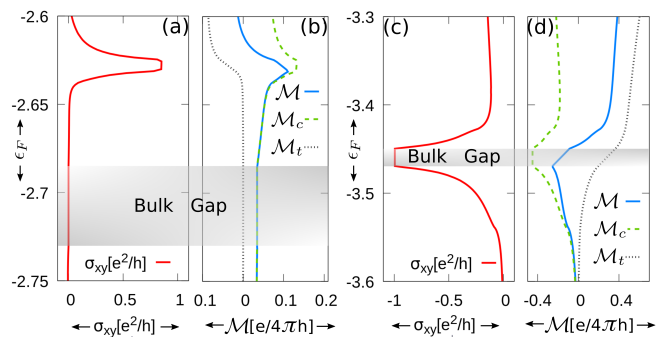


FIG. 3: (Color online) ϵ_F dependence (in units of t) of the topological Hall conductivity σ_{xy} (panels (a) and (c)), exhibiting a transition from zero to quantized value in the bulk gap window as a function of Fermi energy. Panels (b) and (d) show the orbital magnetization \mathcal{M} (and $\mathcal{M}_c, \mathcal{M}_t$) in units of $[e/4\pi\hbar]$. The shaded areas correspond to the energy gap Δ_1 .

low field to a quantized value $\sigma_{xy} = -\frac{e^2}{h}$ at high field (Fig. 3a and 3c). This is confirmed by the calculation of the Chern number where the lowest band is topologically trivial with $C_1 = 0$ at low field and non-trivial with $C_1 = -1$ at high field. This topological change is also evidenced in the orbital magnetization (Eq. 6). In Fig. 3(panel b and d) we show the orbital magnetization (\mathcal{M}) and its two components \mathcal{M}_c and \mathcal{M}_t as a function of ϵ_F . On one hand, we observe that in the energy gap, at low field there is only a negative contribution from the conventional part \mathcal{M}_c . Because $C_1 = 0$ we have $\mathcal{M}_t \equiv 0$. On the other hand, at high field, \mathcal{M}_c keeps constant inside the gap, due to the fact that the integral of m_n^z does not depend on ϵ_F . In contrast, the Berry-phase term \mathcal{M}_c linearly increases with ϵ_F , as is expected from Eq. (6).

In order to inspect in more detail the effects of the transition, we calculate the electronic occupation $n_{\mathbf{r}} = \langle u_1(\mathbf{k}) | \hat{d}_{\mathbf{r}}^\dagger \hat{d}_{\mathbf{r}} | u_1(\mathbf{k}) \rangle$ within the unit cell at Γ point for the lowest band for $B/J = 2.4$ and 4.6 . In the low-field region it is strongly confined around the anti-ferromagnetic skyrmion center in a ring-like configuration[49] (Fig. 4a). As we cross the transition the electronic occupation spreads out, getting away from the skyrmions centers, forming a connected configuration throughout the system (Fig. 4b). This localized/delocalized like transition is compatible with the change in Hall conductivity.

Lastly, we study the presence of in-gap chiral edge states. To this end, we have numerically diagonalized the Hamiltonian Eq. (3) in a one-dimensional strip configuration with a width of 20 unit cells. The calculated band structure with periodic and open boundary conditions is shown in Fig. 4c. In the high-field region, a gap crossing edge state, absent in the low field region, is observed. The electronic occupation for this state localizes in the edge of the sample, as shown in Fig. 4d. A similar behaviour can be found in the persistent energy gap Δ_2 with stable in-gap chiral edge states (see Supplemental

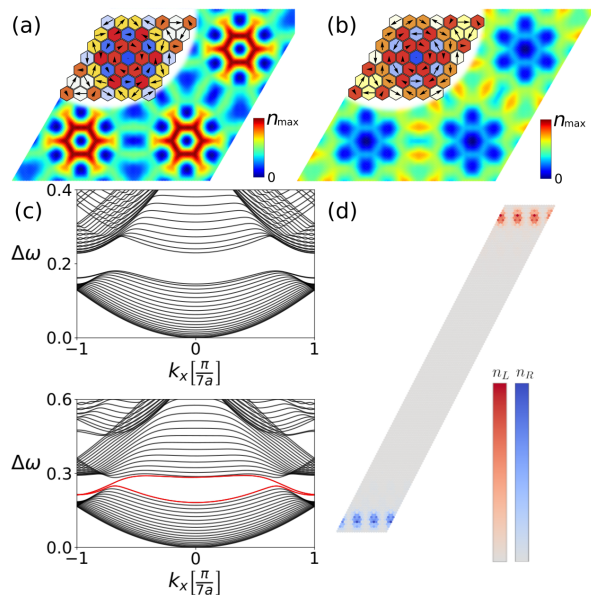


FIG. 4: (Color online) Electronic occupation at the Γ point for the lowest band for $B/J = 2.4$ (a) and $B/J = 4.6$ (b). In the trivial case ($C_1 = 0$) the electron density is strongly localized inside the AF-Skyrmion; when $C_1 = -1$ it becomes delocalized (the top-left insets show the spin configurations). (c) One dimensional band structure ($\Delta w = \epsilon_n - \epsilon_1$ in units of t) for a nanoribbon geometry with periodic (upper) and open (bottom) boundary conditions. In the last case, the edge state (red curve) is clearly observed between the two adjacent bands, which demonstrates a nonzero Chern number. (d) The edges states are localized at the boundary (top and bottom) of the nanoribbon.

Material [40], Sec. II, Fig. 2). This result agrees with the bulk-boundary correspondence principle.

Therefore, a system of this kind with a filled first band could be tuned from an insulator, to a metal, to a Chern insulator phase by changing the external magnetic field. Edge conducting states can be turned on and off in the same manner.

High filling sector.— At high filling, the band structure, Hall conductivity and orbital magnetization show a striking similarity to that observed in ferromagnetic skyrmion crystals [32, 50] as function of the Fermi energy (see Fig. 5). The presence of THE is a consequence of the three sublattice structure of the AF-SkX magnetic background. On an AF-SkX on a bipartite lattice one would expect the emergent field to fluctuate around zero, leading to a vanishing Hall conductivity [37]. However, in the case of the AF-SkX on the triangular lattice, the emergent field fluctuates around a non-zero value and its strength is comparable to that of the emergent field coming from a ferromagnetic Skyrmion lattice background. In this sense, a correspondence between the Integer Quantum Hall Effect and the THE on the AF-SkX could be traced, as is the case of ferromagnetic Skyrmion lattices [32].

Conclusions.— In this letter we have studied the Topo-

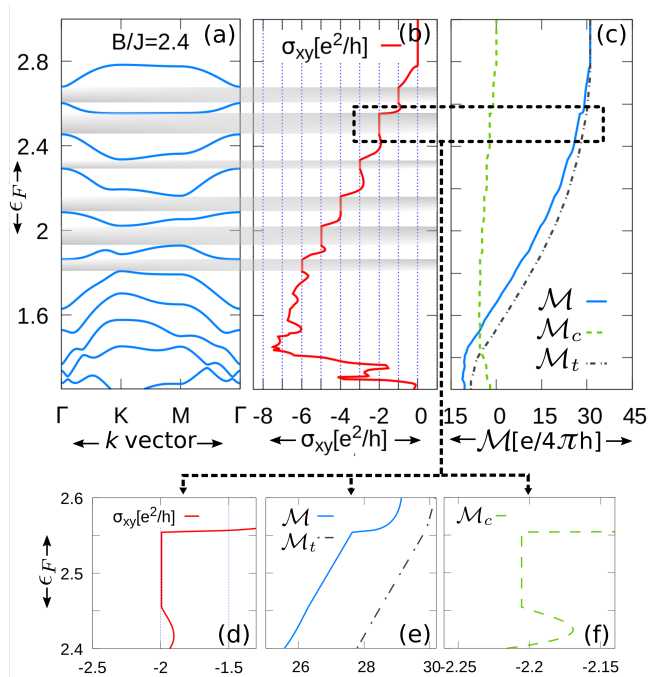


FIG. 5: (Color online) (a) Electronic band structure at high filling band (in units of t), (b) Hall conductivity and (c) orbital magnetization as a function of the Fermi energy (vertical axis). Regions with bulk gap are indicated by a gray rectangular box. In panels (d),(e) and (f) we show a zoomed region in order to highlight the connection between quantities.

logical Hall Effect and Orbital Magnetism of electrons coupled to an antiferromagnetic skyrmion lattice. The band structure consists of two energy regions, separated by a persistent energy gap. The low-energy sector consists of a strongly overlapping bands except for a switchable bulk gap between the first and second band. The high-energy sector shows striking similarity to that of the Integer Quantum Hall Effect.

At low-filling, we found that a magnetic field drives the system from a conventional insulating state to a topological insulator state hosting chiral edge states in generic strip geometries. This topological change is clearly manifested in the Chern numbers, the electron density, Hall conductivity and orbital magnetization. In the region with Chern number $C_1 = 0$, the electron density is strongly localized at the AF-Skyrmion cores forming a ring-like distribution. In the region with $C_1 = -1$, it becomes delocalized. We found that the localization/delocalization of the ring states can be controlled by the magnetic field which determines the texture details. The Hall conductivity presents a switchable behaviour from a null to a quantized value $\sigma_{xy} = -e^2/h$ when the Fermi energy is inside the bulk gap. We have found that the two parts \mathcal{M}_c and \mathcal{M}_t of the orbital magnetization displays a fully different behaviors in the $C_1 = 0$ and $C_1 = -1$ regions because of their different roles in these

two regions.

At high fillings, even having a three sublattice structure of the AF-SkX we recover a similar behavior observed in a ferromagnetic Skymion lattice where it is possible to connect the THE with the Integer Quantum Hall Effect.

Our results highlight the richness of the electronic phases arising from systems hosting AF-SkX states and their potential as platforms for spintronic devices. The present study on the THE in antiferromagnetic skyrmion lattices calls for experimental verification. The low filling topological phase transition and controlled chiral edge states can be studied in materials which exhibit a AF-SkX phase, e.g., the recent fractional skyrmion lattice observed in the compound MnSc_2S_4 [23]. In this material, magnetic ions Mn^{2+} form a diamond lattice. At low temperature and finite magnetic field, each triangular lattice layer along the [111] direction realizes a fractional AF-SkX that is composed of three ferromagnetic Skymion sublattices.

Acknowledgments. – We thank Pierre Pujol for valuable comments. H.D.R thanks Flavia Gómez Albarracín for fruitful discussions. This work was partially supported by CONICET (PIP 2015-813), ANPCyT (PICT 2012-1724) and SECyT-UNLP (PPID X039). H.D.R. acknowledges support from PICT 2016-4083.

-
- [1] N. Nagaosa and Y. Tokura, *Nature nanotechnology* **8**, 899 (2013).
- [2] A. Fert, V. Cros, and J. Sampaio, *Nature nanotechnology* **8**, 152 (2013).
- [3] S. Mühlbauer, B. Binz, F. Jonietz, C. Pfleiderer, A. Rosch, A. Neubauer, R. Georgii, and P. Böni, *Science* **323**, 915 (2009).
- [4] F. Jonietz, S. Mühlbauer, C. Pfleiderer, A. Neubauer, W. Münzer, A. Bauer, T. Adams, R. Georgii, P. Böni, R. A. Duine, *et al.*, *Science* **330**, 1648 (2010).
- [5] X. Yu, N. Kanazawa, Y. Onose, K. Kimoto, W. Zhang, S. Ishiwata, Y. Matsui, and Y. Tokura, *Nature materials* **10**, 106 (2011).
- [6] X. Yu, Y. Onose, N. Kanazawa, J. Park, J. Han, Y. Matsui, N. Nagaosa, and Y. Tokura, *Nature* **465**, 901 (2010).
- [7] Y. Tokunaga, X. Yu, J. White, H. M. Rønnow, D. Morikawa, Y. Taguchi, and Y. Tokura, *Nature communications* **6**, 1 (2015).
- [8] S. Seki, X. Yu, S. Ishiwata, and Y. Tokura, *Science* **336**, 198 (2012).
- [9] S. Seki, S. Ishiwata, and Y. Tokura, *Physical Review B* **86**, 060403 (2012).
- [10] A. N. Bogdanov and D. Yablonskii, *Zh. Eksp. Teor. Fiz* **95**, 178 (1989).
- [11] A. Bogdanov and A. Hubert, *Journal of magnetism and magnetic materials* **138**, 255 (1994).
- [12] A. Bocdanov and A. Hubert, *physica status solidi (b)* **186**, 527 (1994).
- [13] U. K. Roessler, A. Bogdanov, and C. Pfleiderer, *Nature* **442**, 797 (2006).
- [14] H. D. Rosales, D. C. Cabra, and P. Pujol, *Physical Review B* **92**, 214439 (2015).
- [15] J. Barker and O. A. Tretiakov, *Physical review letters* **116**, 147203 (2016).
- [16] X. Zhang, Y. Zhou, and M. Ezawa, *Scientific reports* **6**, 24795 (2016).
- [17] H. Fujita and M. Sato, *Physical Review B* **95**, 054421 (2017).
- [18] C. Jin, C. Song, J. Wang, and Q. Liu, *Applied Physics Letters* **109**, 182404 (2016).
- [19] S. A. Osorio, H. D. Rosales, M. B. Sturla, and D. C. Cabra, *Physical Review B* **96**, 024404 (2017).
- [20] S. Osorio, M. Sturla, H. Rosales, and D. Cabra, *Physical Review B* **99**, 064439 (2019).
- [21] S. Osorio, M. Sturla, H. Rosales, and D. Cabra, *Physical Review B* **100**, 220404(R) (2019).
- [22] M. Villalba, F. Gómez Albarracín, H. Rosales, and D. Cabra, *Physical Review B* **100**, 245106 (2019).
- [23] S. Gao, H. D. Rosales, F. A. G. Albarracín, V. Tsurkan, G. Kaur, T. Fennell, P. Steffens, M. Boehm, P. Čermák, A. Schneidewind, *et al.*, *Nature* **586**, 37 (2020).
- [24] A. Neubauer, C. Pfleiderer, B. Binz, A. Rosch, R. Ritz, P. Niklowitz, and P. Böni, *Physical review letters* **102**, 186602 (2009).
- [25] T. Schulz, R. Ritz, A. Bauer, M. Halder, M. Wagner, C. Franz, C. Pfleiderer, K. Everschor, M. Garst, and A. Rosch, *Nature Physics* **8**, 301 (2012).
- [26] N. Kanazawa, Y. Onose, T. Arima, D. Okuyama, K. Ohoyama, S. Wakimoto, K. Kakurai, S. Ishiwata, and Y. Tokura, *Physical review letters* **106**, 156603 (2011).
- [27] M. Lee, W. Kang, Y. Onose, Y. Tokura, and N. P. Ong, *Physical review letters* **102**, 186601 (2009).
- [28] Y. Li, N. Kanazawa, X. Yu, A. Tsukazaki, M. Kawasaki, M. Ichikawa, X. Jin, F. Kagawa, and Y. Tokura, *Physical review letters* **110**, 117202 (2013).
- [29] P. Bruno, V. Dugaev, and M. Taillefumier, *Physical review letters* **93**, 096806 (2004).
- [30] P. B. Ndiaye, C. A. Akosa, and A. Manchon, *Physical Review B* **95**, 064426 (2017).
- [31] H. Rosales, F. Gómez Albarracín, and P. Pujol, *Physical Review B* **99**, 035163 (2019).
- [32] B. Göbel, A. Mook, J. Henk, and I. Mertig, *Physical Review B* **95**, 094413 (2017).
- [33] B. Göbel, A. Mook, J. Henk, and I. Mertig, *New Journal of Physics* **19**, 063042 (2017).
- [34] B. Göbel, A. Mook, J. Henk, and I. Mertig, *The European Physical Journal B* **91**, 179 (2018).
- [35] W. Jiang, X. Zhang, G. Yu, W. Zhang, X. Wang, M. B. Jungfleisch, J. E. Pearson, X. Cheng, O. Heinonen, K. L. Wang, *et al.*, *Nature Physics* **13**, 162 (2017).
- [36] B. Göbel, I. Mertig, and O. A. Tretiakov, *Physics Reports* (2020).
- [37] B. Göbel, A. Mook, J. Henk, and I. Mertig, *Physical Review B* **96**, 060406 (2017).
- [38] F. Gómez Albarracín and H. Rosales, *Physical Review B* **93**, 144413 (2016).
- [39] S. A. Díaz, J. Klinovaja, and D. Loss, *Physical review letters* **122**, 187203 (2019).
- [40] See Supplemental Material at [URL] for details related with Monte-Carlo simulations, the spin configurations and magnetic unit cells used for our calculations (section I), the details of the transformation to obtain the effective Hamiltonian of spinless fermions (section II) and figures of the electronic occupation in the energy gap Δ_2 (section

III). .

- [41] S. Reja, arXiv preprint arXiv:2005.02724 (2020).
- [42] K. Ohgushi, S. Murakami, and N. Nagaosa, Physical Review B **62**, R6065 (2000).
- [43] T. Fukui, Y. Hatsugai, and H. Suzuki, Journal of the Physical Society of Japan **74**, 1674 (2005).
- [44] F. Takahiro, H. Yasuhiro, and S. Hiroshi, Journal of the Physical Society of Japan (2013).
- [45] Y. Hatsugai, Physical review letters **71**, 3697 (1993).
- [46] M.-C. Chang and Q. Niu, Physical Review B **53**, 7010 (1996).
- [47] D. Xiao, J. Shi, and Q. Niu, Physical review letters **95**, 137204 (2005).
- [48] A. Raoux, F. Piéchon, J.-N. Fuchs, and G. Montambaux, Physical Review B **91**, 085120 (2015).
- [49] M. Redies, F. Lux, J.-P. Hanke, P. Buhl, S. Blügel, and Y. Mokrousov, arXiv preprint arXiv:2003.03243 (2020).
- [50] K. Hamamoto, M. Ezawa, and N. Nagaosa, Physical Review B **92**, 115417 (2015).